Direct Identification of Three Crystalline Phases in PEO-b-PCL-b-PLLA Triblock Terpolymer by In Situ Hot-Stage Atomic Force Microscopy

Jordana K. Palacios[1-2], Heng Zhang[3], Bin Zhang[3], Nikos Hadjichristidis[4*], Alejandro J. Müller[1,5*]*

[1]POLYMAT and Polymer Science and Technology Department, Faculty of Chemistry, University of the Basque Country UPV/EHU, Paseo Manuel de Lardizabal 3, 20018 Donostia-San Sebastián, Spain.

[2] Fundación Centro Tecnológico Miranda de Ebro (CTME), R&D Materials Department, Miranda de Ebro, 09200, Burgos, Spain.

[3]School of Materials Science & Engineering, Zhengzhou University, Zhengzhou 450002, People's Republic of China.

[4]King Abdullah University of Science and Technology (KAUST), Physical Sciences and Engineering Division, KAUST Catalysis Center, Thuwal, Saudi Arabia.

[5]IKERBASQUE, Basque Foundation for Science, Bilbao, Spain.

*Corresponding authors: binzhang@zzu.edu.cn, Nikolaos.Hadjichristidis@kaust.edu.sa, alejandrojesus.muller@ehu.es

ABSTRACT

In this work, we provide a detailed description of the tri-lamellar nanoscale morphology of a triple crystalline PEO-*b*-PCL-*b*-PLLA triblock terpolymer obtained by Hot-Stage Atomic Force microscopy (AFM) imaging and Wide Angle X-ray scattering (WAXS) analysis for the first time. The precursor PCL-*b*-PLLA diblock copolymer has also been included in the study for comparison purposes. A two-step crystallization protocol has been applied to create a distinct lamellar morphology. Both WAXS and AFM revealed the double crystalline nature of the diblock copolymer. However, the identification of multiple crystalline phases in the triblock terpolymer by AFM and WAXS at room temperature is not straightforward. The advantages of hot-stage AFM allowed following the evolution of the lamellar morphology and the successive melting of the tricrystalline PEO-*b*-PCL-*b*-PLLA sample during heating. Taking into account the melting temperature of each crystalline block, the existing lamellar populations were clearly identified. At 45 °C, the thinnest lamellae disappeared, due to the melting of PEO crystals. The medium size lamellae disappeared at 60 °C when PCL crystals melt. At that temperature, the only remaining crystals are those of the PLLA block. AFM mechanical modulus images and the analysis of the cross-sectional heights provide further evidence of the lamellar self-assembly of the triblock terpolymer. It was found that two lamellar arrangements are possible at room temperature; either a perfect interdigitation where PCL and PEO lamellae are sandwhiched between PLLA lamellae (i.e., PLLA/PEO/PCL/PLLA), or only one PEO or PCL lamella in between two PLLA lamellar crystals distributed randomly (i.e., PLLA/PEO/PLLA or PLLA/PCL/PLLA). Hot-Stage AFM is a valuable technique to elucidate the complex morphological features of multi-crystalline systems.

Keywords: PEO-*b*-PCL-*b*-PLLA triblock terpolymer; tri-lamellar morphology; Hot-Stage AFM; WAXS

INTRODUCTION

The morphology of block copolymers has attracted broad interest in the polymer scientific community in the last decade. The micro and nanostructural features are influenced by several factors, such as melt miscibility, crystallinity, composition, and thermal conditioning. A wide range of different morphologies can be developed that depend on whether the block copolymer is miscible or melt segregated, or if it is amorphous, semicrystalline or combined (double crystalline, double amorphous, crystalline-amorphous, etc.) [1-7].

To study the morphology of block copolymers in real space, a series of techniques can be used, such as polarized light optical microscopy (PLOM), transmission electron microscopy (TEM), and atomic force microscopy (AFM). Among them, AFM is an imaging technique of high-resolution that not only substantially complements the interpretation of TEM and PLOM observations but also of other structural characterization techniques in reciprocal space, such as X-ray diffraction. AFM allows direct visualization of the nanoscale structure. However, it should be kept in mind that AFM is a surface technique, and it might not represent bulk structural behavior[8-10].

AFM has been used to detect microphase-separated morphologies of block copolymers. Block copolymers display different morphologies depending on three main factors: copolymer composition and architecture, melt segregation strength, and thermal transitions (e.g., order-disorder, crystallization, and glass transition temperatures) [3, 5]. The ordered superstructure sizes range from micro to nanoscale level. For instance, AFM has been useful to detect several types of microdomain patterns in strongly segregated

systems [11, 12], as well as, lamellar nanodomains in weakly segregated or melt miscible systems. Particularly, melt miscible (or weakly segregated) block copolymers with crystallizable blocks, the final morphology is a consequence of the crystallization conditions and the microphase segregation driven by the crystallization event. AFM examinations at room temperature reveal the self-assembly of the polymer chains into mixed axialitic or spherulitic-type superstructures composed of lamellar arrangements [2, 6, 7, 13-30].

A group of well-investigated melt miscible (or weakly segregated) double crystalline systems are the diblock and triblock copolymers composed of poly(L-lactide) (PLLA), poly(caprolactone) (PCL) and poly(ethylene oxide) (PEO) due to their good physical properties and biodegradability. Extensive research has been published regarding their microscale morphology. Spherulites, banded or concentric spherulites, axialities, 2D aggregates, among others crystalline textures, have been reported [26, 29, 31-35].

For a few years, we have been investigating the complexity of the morphology and crystallization of unique ABC triblock terpolymers, in which the three blocks are able to crystallize when the length of the blocks and the crystallization conditions are adjusted properly. To that purpose, model triblock terpolymers of PLLA, PCL, and PEO blocks (PEO-*b*-PCL-*b*-PLLA) have been exhaustively studied [4, 35-38]. Particularly, the morphology of these melt miscible and triple crystalline triblock terpolymers have been reported by Chiang et al.[39] and Palacios et al.[35, 37, 38]. Wide-angle X-Ray scattering (WAXS) measurements, carried out during cooling, confirmed that the PLLA block is the one that crystallizes first, followed by the PCL and lastly, the PEO. PLOM observations indicated that the microscale structure is templated by the PLLA block as a result of its

crystallization. The successive crystallization of the PCL and PEO blocks does not change the microscale superstructure templated by the PLLA block. The evidence of the crystallization of the other two blocks is that the magnitude of the birefringence varies [35]. Linear and cyclic diblock copolymers of PCL, PLLA and PEO also exhibit this behavior [13, 33, 34, 40-45]. Chiang et al.[39] presented single crystals of PEO-*b*-PCL-*b*-PLLA triblock terpolymers crystallized from solution.

Some features of the triple crystalline nanoscale morphology of PEO-*b*-PCL-*b*-PLLA triblock terpolymers have been reported by some of us in a previous publication [37]. A tri-lamellar self-assembly that included lamellae of the three phases was indirectly elucidated from AFM observations at room temperature, complemented with SAXS experiments and theoretical simulations. From our observations, we proposed a lamellar arrangement that includes the alternation of only one lamella of either PCL or PEO in between two lamellae of PLLA. However, a clear identification of such peculiar variation of the lamellar crystalline phases was not possible by only room temperature AFM observations. Therefore, the next step would be to apply a thermal scan to the lamellar morphology observed at room temperature to get further insight into the tri-lamellar structure and long-range order.

AFM advantages include that the measurements can be extended from room to higher temperatures. Prilliman et al.[46] reported in 1998 the development of a Hot-Stage AFM in tapping mode. A coupled cooling/heating device allows *in situ* visualization of the morphological changes resulting from thermal transitions. To study phase transitions, images at different temperatures are recorded after the sample has been heated or cooled, or the AFM probe is heated during the heating scan or during the phase transition. [8, 9].

AFM has already been used to image the melting and crystalline morphology during crystallization at high temperatures for polyethylene (PE) [8, 47-49], PCL [50-52], and PEO [53-56]. Additionally, hot-stage AFM has been used to examine PEO / poly(butylene succinate) (PBS) blends with different compositions [57]. The hot-stage AFM technique was useful to determine the local distribution of the crystals and to evaluate the influence of both composition and isothermal crystallization temperature chosen.

Imaging semicrystalline diblock copolymers at high temperatures, employing hot-stage AFM, should provide more insight into the nanoscale lamellar arrangement. However, only a few reports on single and double crystalline diblock copolymers and terpolymers have been published, and most of the AFM polymer crystal observations deal with samples crystallized from solution and only a few with samples crystallized from the melt. In diblock copolymers of PEO containing a tablet-like block of poly(2,5-bis[(4-methoxyphenyl)oxycarbonyl]styrene) (PMPCS) (PEO-*b*-PMPCS) [58], hot-stage AFM has been used to follow the PEO block crystallization. Under isothermal conditions, the PEO crystallized into dendritic structures if the crystallization temperature is lower than 44 °C, but the morphology changed to square-shaped crystals at temperatures higher than 48 °C. By AFM, the authors were also able to determine that the lamellar thickness increased as the crystallization temperature was higher [58]. Hot-stage AFM has also been used by Zhan et al.[59] to examine the relief structure of PS-*b*-PCL diblock copolymers. In these copolymers, the PCL block only crystallized, and the AFM technique was employed to analyze the complex competition between dewetting and microphase separation.

To our knowledge, only Cui et al.[60] and Schmalz et al.[61] have in-situ followed the structural changes upon heating and cooling of AB diblock copolymers and ABC

triblock terpolymers in which only two blocks crystallize. Employing hot-stage AFM, Cui et al.[60] studied the PLLA block crystallization behavior in PCL-*b*-PLLA diblock copolymers upon cooling from melt and upon heating from room temperature. Different crystalline morphologies were observed depending on the crystallization conditions but not a clear distinction between the PCL and PLLA lamellae. In the triblock terpolymer poly(ethylene)-*b*-poly(ethylene-alt-propylene)-*b*-poly(ethylene oxide) (PE-*b*-PEP-*b*-PEO) reported by Schmalz et al.[61], only the PEO and PE blocks can crystallize. The authors employed scanning force microscopy (SFM) with a hot stage to follow the melting of the PEO crystals and the annealing of the crystalline PE lamellar phase. As this is a melt-segregated terpolymer, isolated crystalline nanodomains of the PEO and PE blocks were spotted.

In this paper, we take advantage of the Hot-Stage AFM approach to provide a clear elucidation of the trilayered lamellar morphology of an ABC-type triple crystalline triblock terpolymer. To our knowledge, this is the first time that Hot-Stage AFM is employed to identify three different crystalline phases successfully. The PEO-*b*-PCL-*b*-PLLA is a triblock terpolymer with an alternating superstructure of three crystalline phases, as we had published previously [4, 35-38]. Here, we report the *in situ* hot-stage AFM observations of the sequential melting of isothermally crystallized PEO-*b*-PCL-*b*-PLLA terpolymer. Complementary WAXS analysis is provided to support the AFM evidence. Assessing the distribution of discrete crystals provides a deeper understanding of the sequential crystallization and melting in PEO-*b*-PCL-*b*-PLLA triblock terpolymers.

EXPERIMENTAL PART

Materials

A diblock copolymer precursor (PCL-*b*-PLLA) and a PEO-*b*-PCL-*b*-PLLA triblock terpolymer were selected for the morphological characterization. These materials were synthesized as previously reported by a one-pot sequential organocatalytic ring-opening sequential polymerization of ethylene oxide, ε-caprolactone, and L-lactide. A phosphazene base, 1-tert-butyl-2,2,4,4,4-pentakis-(dimethylamino)-2λ5,4λ5-catenadi(phosphazene) (t-BuP2) was employed as a single catalyst. For more details on the synthesis procedure and characterization, refer to[62, 63], and the references in them.

Table 1. Molecular weight, composition and melting point data of the two samples employed in this work.

Sample code	M_n (gmol^{-1}) PEO block	T_m (ºC) PEO block	M_n (gmol^{-1}) PCL block	T_m (ºC) PCL block	M_n (gmol^{-1}) PLLA block	T_m (ºC) PLLA block	Đ (M_w/M_n)
$PCL_{43}PLLA_{57}^{15.4}$	-		6600	52-55	8800	134-139	1.16
$PEO_{23}PCL_{34}PLLA_{43}^{19.9}$	4600	41-46*	6800	52-57*	8500	120-127*	1.18

*The melting point values reported here are a range because they depend on previous thermal history (controlled cooling or isothermal crystallization) and scanning rates employed during their determination (1, 5 or 20 ºC/min) [33-36].

The PLLA and PCL block length in both terpolymer and diblock copolymer was very similar (see Table 1) to avoid any influence of molecular weight on crystallization. We obtained molecular weight distributions (Đ< 1.20) that can be considered relatively narrow.

Nuclear magnetic resonance spectra (^{1}H NMR) and size exclusion chromatography (SEC) were employed to determine chemical structure and number-average molecular weights (M_n) of the materials and their block components. The samples under study are listed in Table 1, with composition of the blocks as subscript numbers and molecular weights of the entire diblock copolymer and terpolymer as superscript numbers. The melting points of each component determined by DSC previously [33-36] are also given in Table 1.

Film Preparation.

Film samples were prepared by spin coating. The polymers were dissolved in chloroform at room temperature to make 0.1%, 0.2% and 0.5% w/w solutions. The polymer solution was dropped onto a 1 cm^2 Si wafer, which was previously cleaned and oxidized with UV light, and then, it was spin-coated. The film thickness was about 20 nm.

Thermal Treatment to Induce Microphase Separation.

All blocks within the diblock copolymer and triblock terpolymer under study were previously crystallized, employing a two-step crystallization method. To erase thermal history, the sample was first melted at 160 °C for 3 minutes. Then, to crystallize the PLLA block, it was cooled from the melt to 0 ºC at 20 ºC min^{-1} and finally heated up to 81 ºC at 60 ºC min^{-1}. During cooling from the melt, the PLLA block does not crystallize (this has been confirmed before by DSC and WAXS analysis). Due to the slow crystallization kinetics of the PLLA when cooled from the melt, it was decided to crystallize the PLLA block from the glassy state (0 °C). Cooling down to 0 °C provokes an increase in nucleation density of the PLLA as it vitrifies, and therefore, increases its ability to crystallize upon heating from the glassy state (i.e., cold-crystallization). Thus, the PLLA block was

isothermally crystallized to saturation at 81 ºC during 1 h, while the other two blocks were in the molten state.

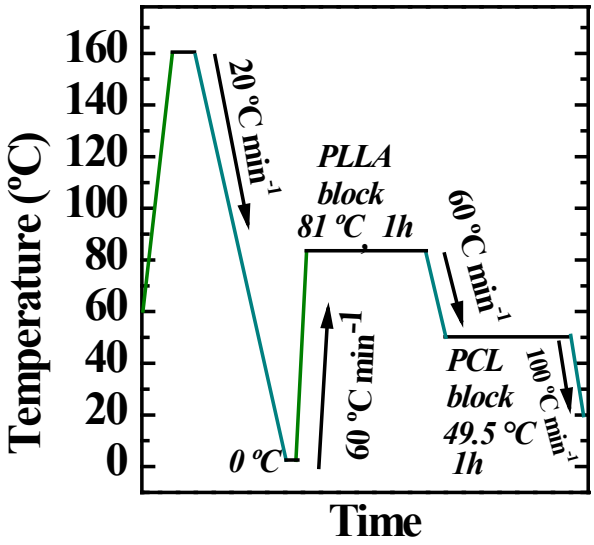

Figure 1. Thermal crystallization protocol with two isothermal steps.

To crystallize the PCL block, the sample was then cooled to 49.5 ºC at 60 ºC min^{-1} and held at this temperature for 1 h to crystllize it until saturation. That temperature induces the PCL block crystallization only, and the PEO block remains molten. Each isothermal step was 1 h to induce the thickest lamellar thickness at these conditions. Finally, the sample was quenched to 25 ºC at 100 ºC min^{-1} (during this last cooling, the PEO block in the triblock terpolymer can crystallize [35], forming the thinnest lamellae of the three components). After this thermal treatment, the samples were examined by AFM and WAXS.

Morphological Observations.

The as-crystallized films were measured with a Dimension Icon microscope (Bruker, USA) equipped with heating accessories. The measurements were performed by ScanAsyst mode with Bruker probes (SCANASYST-AIR mode; 12 nm tip radius; 0.4N/m spring constant and 70kHz resonant frequency) to simultaneously image the microstructure topography and the mechanical properties (i.e., modulus).

To evaluate the microphase separation by atomic force microscopy (AFM) with an *in situ* heating stage, two particular *in situ* thermal protocols were used:

(i) One step heating method. The as-crystallized $PCL_{43}PLLA_{57}^{15.4}$ sample was heated from room temperature (25 °C) to 70 ºC (a temperature above the melting point of the PCL block crystals, see Table 1) at 1 ºC min^{-1} and held at this temperature for *in situ* characterization AFM observations were made at 25 and 70 °C.

(ii) Two steps heating method. The as-crystallized $PEO_{23}PCL_{34}PLLA_{43}^{19.9}$ sample was heated from room temperature (25 °C) to 45 ºC (to melt the PEO block crystals, see Table 1) at a heating rate of 1 ºC min^{-1} and kept at this temperature for *in situ* AFM observations. Subsequently, it was heated up to 60 ºC (to melt the PCL block crystals, see Table 1) also at 1 ºC.min^{-1}, and *in situ* AFM characterization was again performed to image the PLLA block crystals. Thus, observations were made at 25, 45, and 60 °C.

Wide Angle X-ray Scattering (WAXS) experiments.

WAXS experiments were carried out on films of the samples that were previously subjected to the crystallization protocol described earlier. The WAXS scattering patterns were acquired *in situ* to follow the evolution of the microphase separation as the samples

were heated. The *in situ* WAXS measurements were conducted in the ALBA Synchrotron Radiation Facility (Cerdanyola del Valles, Barcelona, Spain) (beamline BL11-NCD). A Rayonix LX255-HS detector with a resolution of 1920 × 5760 pixels (pixel size: 40 μm^2) was employed to record the WAXS patterns on heating. Silver behenate and Cr_2O_3 standards were used to perform the calibration. The physical parameters were the following: tilt angle, 30°; effective scattering vector q range, 8−22 nm^{-1}; and sample-to-detector distance; 126.8 mm. The radiation source had a wavelength (λ) of 0.9999 Å. The DAWN software was used to process the data and to produce intensity plots as a function of the scattering vector, q ($q = 2\pi/d = 4\pi \sin \theta/\lambda$). The temperature was controlled employing a Linkam Scientific Instruments THMS600 hot-stage with a liquid nitrogen cooling system. WAXS patterns were recorded on heating between 25 and 160 °C. The heating rate was set at 5 °C min^{-1}. An acquisition time of 6 s was used for each pattern. Thus, the temperature resolution was 0.5 °C. The WAXS patterns are presented between 1 and 2 A^{-1}. In this range, most crystallographic reflections of the blocks species under study are observed.

RESULTS AND DISCUSSION

Two samples were selected in this work, a $PEO_{23}PCL_{34}PLLA_{43}^{19.9}$ triblock terpolymer and its precursor, a $PCL_{43}PLLA_{57}^{15.4}$ diblock copolymer, as they can be regarded as model di and triblock copolymer and terpolymer samples with crystallizable blocks. Both samples are most probably melt miscible. SAXS observations in the melt showed no scattering [35, 37], although the electron density between these blocks is quite

similar [28]. Upon cooling from the melt, both DSC and WAXS analysis showed that the two phases in the diblock and the three phases in the triblock crystallized [35].

An image of this tri-lamellar morphology at room temperature observed by AFM has been published by us before [37]. However, we could not observe the morphology by AFM as the sample was heated. In this work, on the other hand, by employing *in situ* hot-stage AFM, we are able to show the presence of the three clear, distinct phases and corroborate the DSC and WAXS observations. Samples were prepared by spin coating employing different solution concentrations to determine the best sample preparation conditions. The samples were subjected to a thermal protocol that includes two isothermal steps to induce each block crystallization until saturation.

The as-crystallized samples (following the protocol of Figure 1) were observed by AFM at 25 °C and during a subsequent heating scan employing a hot-stage. Two thermal protocols were employed: one step heating scan, in which AFM observations were made at 25 and 70 °C, and a two-step heating scan, in which the observations were made at 25, 45, and 60 °C.

The alternated morphology of the PCL-b-PLLA diblock copolymer

The nanoscale morphology of the $PCL_{43}PLLA_{57}^{15.4}$ diblock copolymer was examined first. Figure 2 shows AFM height images of a sample prepared initially by spin-coating from solution but then subjected to the thermal crystallization protocol indicated in Figure 1. Figure 2a and b show the lamellar structure at 25 °C before applying the one-step heating scan. Most of the lamellae have grown in an edge-on fashion, allowing lamellar thickness measurements.

Figure 3a shows for the $PCL_{43}PLLA_{57}^{15.4}$ diblock copolymer sample, several packed lamellae that include alternated PCL and PLLA blocks lamellae. After careful observation and measurements of the AFM micrographs, two populations of different lamellar thickness were identified. One of them has an average thickness of 15 ± 1 nm, indicated with red dotted lines and the other, of 10 ± 1 nm, indicated with green dotted lines (Figure 2b). These values agree well with our previous report on the lamellar structure of these copolymers [37]. In that report [37], the AFM observations were made by Multimode Scanning Probe Microscope (tapping mode) and using microfabricated silicon tips/cantilevers. We established that the thickest lamellae (15 nm, red) should belong to the PLLA block because this block is the one that crystallizes first, while the thinnest lamellae (10 nm, green) should belong to the PCL block.

A WAXS experiment of the as-crystallized sample taken at 25 °C confirmed the presence of both types of crystals (see Figure 3a). The characteristic crystallographic planes of the α-form of the PLLA crystals (110/200 and 113/203) can be observed, as well as, the 110, 111 and 200 reflections of the PCL crystals. However, and until now, it was not possible to assign without doubts to which block correspond each lamellar thickness.

Based on the different melting temperatures of each block (the PCL block melts at around 55 °C and PLLA block at around 120 °C, see Table 1 and our previous work [37]), the premise is that if the sample is heated until a temperature above the melting point of the PCL lamellae but sufficiently low to keep the PLLA phase crystallized, we should be able to see the disappearance of the PCL phase, while the PLLA lamellae will remain intact.

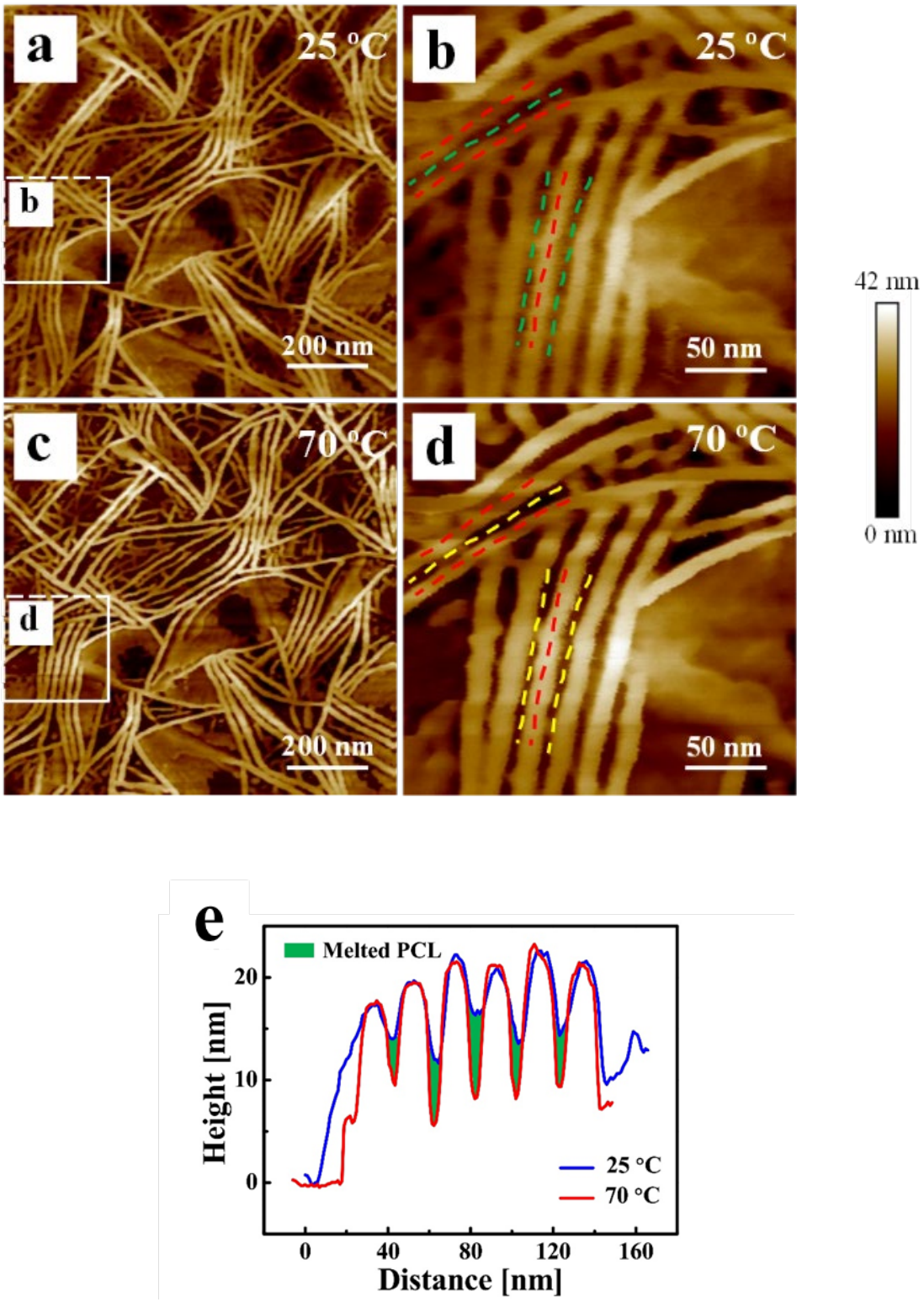

Figure 2. AFM height images of a $PCL_{43}PLLA_{57}$[15.4] sample prepared initially by spin-coating from a 0.2 wt% solution and then subjected to the thermal crystallization protocol

indicated in Figure 1. Images are given at 25 ºC (a, b) and at 70 ºC (c, d) after the heating protocol. The dotted lines indicate PCL lamellae (green), PLLA lamellae (red), and molten PCL regions (yellow). (e) Cross-sectional height profiles along the directions indicated in Figure S1 in the supplementary information. The green regions of height reduction represent molten PCL.

Thus, to confirm the melting transitions of the $PCL_{43}PLLA_{57}^{15.4}$ diblock copolymer, the as-crystallized sample (according to the protocol of Figure 1) was heated up, and simultaneous WAXS measurements were taken during heating.

It can be seen in Figure 3b that at 25 °C, both PCL, and PLLA phases are present. But beyond 60 °C, the reflections of the crystallographic planes of the PCL disappeared due to the melting of the crystals while the PLLA crystals remained unmolten. The PLLA phase melts completely at 160 °C (see Figure 3c).

The as-crystallized sample was carefully heated (1 °C/min) up to 70 °C, and AFM observations at that temperature were performed. Unlike our previous report [35], the AFM used on this occasion consists of a Dimension Icon microscope equipped with a hot-stage device that allows heating the sample *in situ* at a very low heating rate.

Figure 2c and d show the lamellar structure of the $PCL_{43}PLLA_{57}^{15.4}$ diblock copolymer after heating the sample to 70 °C (a temperature above the melting point of the PCL block crystals). Comparing Figure 2b (at 25 °C) and Figure 2d (at 70 °C), it is apparent that the smaller size lamellae (10 nm, green) disappeared as a consequence of the melting of the PCL lamellae. Darker regions (indicated with yellow dot lines) can now be observed in between the bigger size lamellae that remained unchanged. These darker interlamellar regions correspond to the amorphous PCL phase that at 70 °C is molten. In

fact, at this temperature, only PLLA reflections are observed in the WAXS spectrum (see Figure 3b).

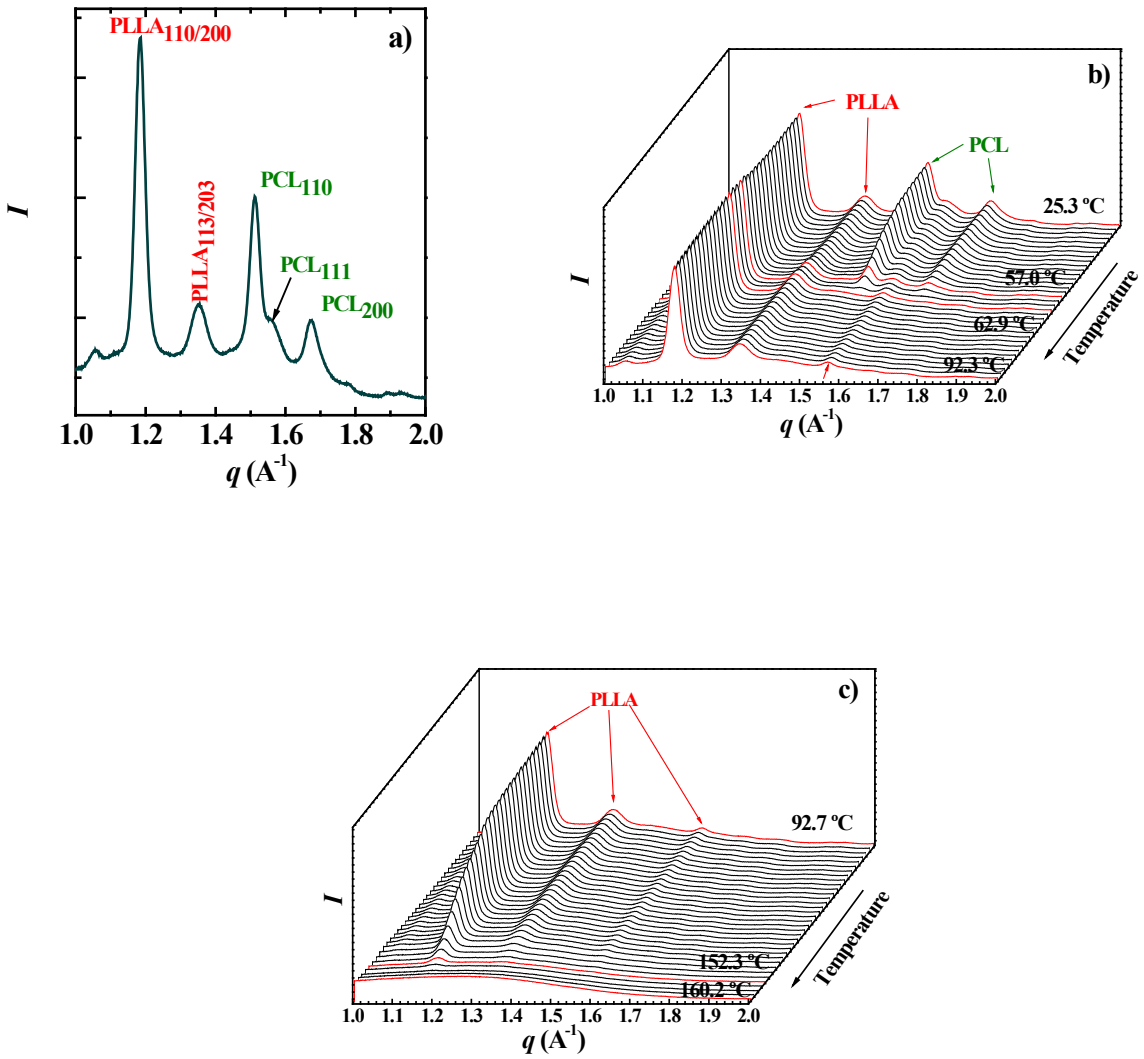

Figure 3. WAXS patterns of $PCL_{43}PLLA_{57}^{15.4}$ diblock copolymer taken at 25 °C, after crystallizing the sample in two isothermal steps (a). WAXS patterns evolution of $PCL_{43}PLLA_{57}^{15.4}$ during subsequent heating between 25 and 92 °C (b) and between 92 and 160 °C (c).

Further and clearer evidence of the lamellar identification and the melting sequence is given in Figure 2e. The height profiles of a section of Figure 2b and d are provided (see

Figure S1 in supplementary information to observe the marked section where the measurements were taken). The cross-sectional height profile at 25 °C (blue line) is composed of alternated peaks and valleys in a regular manner. At that temperature both PCL and PLLA crystals coexist. The peaks correspond to larger size lamellae that belong to the PLLA block. As the temperature is increased up to 70 °C, the height and position of the peaks remain constant while the minima of the valleys decrease (see red line). As it has been stablished, at 70 °C the PCL block is molten. Hence, this variation in the height of the valleys accounts for the melting of interdigitated PCL lamellae (green zone in Figure 2). This is a clear evidence of the alternated lamellar self-assembly. Therefore, the lamellar structure observed at 70 °C corresponds to PLLA lamellae, which are 15 nm in thickness. The PCL-*b*-PLLA diblock copolymer indeed exhibited a double crystalline morphology that includes lamellae of both PCL and PLLA at room temperature.

Cui et al.[60] have previously reported the morphology of PCL-*b*-PLLA diblock copolymers employing a hot-stage AFM. However, the authors did not report a lamellar structure. On the contrary, at 25 °C, a wormlike co-continuous morphology of the blocks was proposed. However, the WAXS analysis demonstrated that only PCL crystals were present at room temperature. As the sample was heated, the PCL crystals melted, and the PLLA crystals started to grow, as confirmed by WAXS. The authors claimed that the wormlike structure was deformed due to the emergence of PLLA lamellae. However, a truly lamellar arrangement is not clear from the AFM images presented. Cooling from the melt to 80 °C, a spherulitic-type texture seemed to emerge as a consequence of PLLA crystallization. Subsequent cooling to 27 °C induced the PCL block crystallization, and the morphology was slightly changed. However, the crystalline structure is not clear [60].

These observations demonstrate the importance of a suitable sample preparation method and crystallization protocol to promote a clear lamellar crystalline morphology.

Besides AFM techniques, the nanoscale lamellar morphology of PLLA-*b*-PCL diblock copolymers has also been observed in the literature by other microscopic techniques. In a previous report from Ho et al.[64], the authors observed by TEM the morphology of crystals that have been crystallized from melt and grown epitaxially. They presented a lamellar phase-separated structure that included both crystalline flat-on PLLA branched lamellae and alternating amorphous layers containing both PCL and PLLA chains. Casas et al.[65], on the other hand, reported solution grown single crystals of PCL-*b*-PLLA diblock copolymers that were observed by TEM. Depending on the crystallization conditions, very complex crystalline morphologies were developed.

Further evidence of the alternated lamellar structure and phase assignment can be provided by the Dimension Icon Microscope employed in this work. This AFM device gives an image of the microstructural topography and at the same time determines the mechanical properties of the sample surface. Thus, properties such as adhesion and modulus can be scanned and mapped in the sample area.

The as-crystallized sample (crystallized as explained in Figure 1) consists of different phases that include PCL and PLLA crystalline phases and a mixed amorphous phase (containing both PCL and PLLA blocks chains) that surrounds the crystalline lamellae (i.e., darker zones around an in-between crystalline lamellae). These three phases should exhibit a different mechanical response. For instance, the amorphous phase is softer than the crystalline one. And between PCL and PLLA, the mechanical features are also

different. In general, tensile modulus values between 3000 and 4000 MPa have been reported for PLA [66], while PCL has been described as a softer material with modulus around 300-400 MPa [67]. Hence PLA is a more rigid material than PCL. Taking all this into consideration, the mechanical performance of the sample was determined employing the Dimension Icon Microscope AFM. Figure 4 shows the AFM modulus images of the $PCL_{43}PLLA_{57}^{15.4}$ sample, initially prepared by spin-coating from solution, and then subjected to the thermal crystallization protocol indicated in Figure 1.

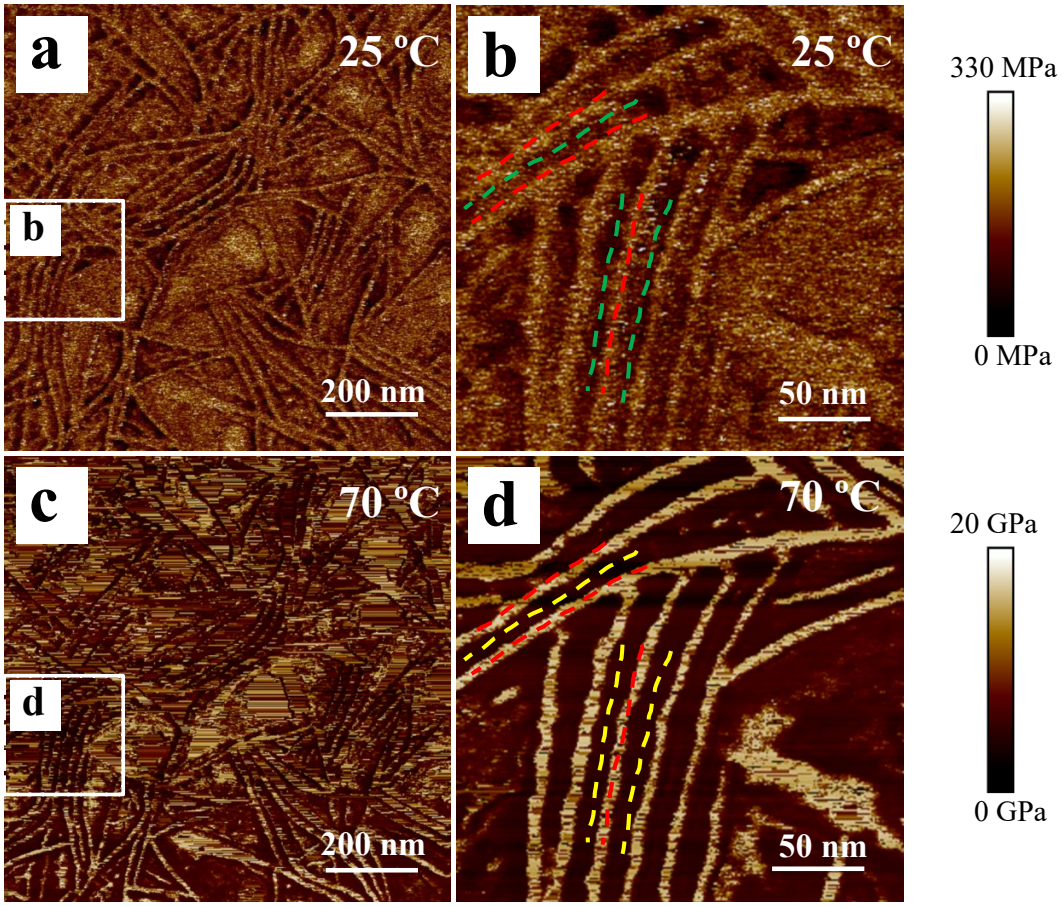

Figure 4. AFM modulus images of a $PCL_{43}PLLA_{57}^{15.4}$ sample, originally prepared by spin-coating from a 0.2 wt% solution, and then subjected to the thermal crystallization protocol indicated in Figure 1. Images are given at 25 ºC (a, b), and at 70 ºC (c, d) after the heating. The dotted lines indicate PCL lamellae (green), PLLA lamellae (red) and molten PCL regions (yellow).

At 25 °C (see Figure 4a and b), identification of the phases present can be made by taking into consideration the modulus values. If relative comparisons are made without taking into account the absolute values, a tentative assignment can be made as the brighter lamellae (of higher modulus) should correspond to the PLLA block (indicated with a red dotted lines) while less bright regions in between PLLA lamellae should be assigned to the PCL lamellae (green dotted line). However, this assignment is confirmed when the sample is heated to 70 °C (see Figure 4d). At that temperature, only the PLLA crystals remain, and the PCL lamellae have melted. Therefore, the very bright lamellae of high modulus are characteristic of the more rigid PLLA crystals. The PLLA lamellae remained unchanged and at the exact position as they were marked with red dotted lines in Figure 4b. On the contrary, the interlamellar PCL block regions appeared completely dark, indicating much lower values of elastic modulus than those in the PLLA block region. Being the amorphous phase a softer one, that observation is an indication of the melting of PCL lamellae and a clear evidence of the alternated lamellar structure, in which the PCL lamellae locates in an interdigitated fashion between the PLLA lamellae when it crystallizes within the previously formed PLLA spherulitic or axialitic templates.

The interlamellar self-assembly of the PEO-b-PCL-b-PLLA triblock terpolymer

Following the same approach employed for the diblock copolymer, the particular interlamellar arrangement of a tri-crystalline PEO-*b*-PCL-*b*-PLLA triblock terpolymer was studied. The sample selected, the $PEO_{23}PCL_{34}PLLA_{43}^{19.9}$, is a triblock terpolymer with the same PLLA and PCL block lengths as in the previously discussed diblock copolymer.. Thus, comparisons between the triblock terpolymer and the diblock copolymer (which is

the precursor of the triblock terpolymer) can be made without any influence of molecular weights of the blocks under consideration.

The complexity of the nanoscale morphology of triblock terpolymers is high when the three blocks are able to crystallize. In our previous reports [35, 37], we demonstrated by DSC and WAXS that the three blocks in $PEO_{23}PCL_{34}PLLA_{43}^{19.9}$ are able to crystallize, and the SAXS analysis indicated that the terpolymer is probably melt miscible. Upon cooling from melt, PLOM and WAXS experiments confirmed that PLLA crystallizes first, creating a spherulitic superstructural template. Then, the next block to crystallize is the PCL block, and the last one is the PEO block. The templated morphology did not change during the successive crystallization of the other PEO and PCL blocks, and only a slight change in the magnitude of the birefringence was observed. Therefore, after crystallization, the lamellae of the three blocks should coexist together in an alternated fashion. To confirm this hypothesis, we applied the crystallization protocol of Figure 1 to the $PEO_{23}PCL_{34}PLLA_{43}^{19.9}$ sample. The crystallization temperatures were chosen to be sufficiently high to induce the crystallization of each block sequentially and separately, and avoid the crystallization of the other two blocks. [37].

In our previous report [37], we were able to identify three different lamellar thicknesses by AFM (15, 10, and 7 nm), and we hypothesized about their origin. The thickest lamellae of 15 nm should belong to the PLLA block because this value was similar to that of the PLLA block in the analogous diblock copolymer, and both blocks have the same molecular weight and were crystallized under identical conditions (i.e., at 81 °C for 1 h). Then, the 10 nm lamellae were assigned to the PCL block due to the same reasons mentioned above. Finally, the smallest lamellae should belong to the PEO block. But, to

prove that, we had to run some WAXS measurements at room temperature and on heating to confirm the presence of PEO crystals. Both PLLA and PEO reflections were observed. However, some reflections of PLLA and PEO crystals overlap (more details are in [37]). Therefore, after the WAXS experiment, the presence of the PEO crystals could only be indirectly confirmed.

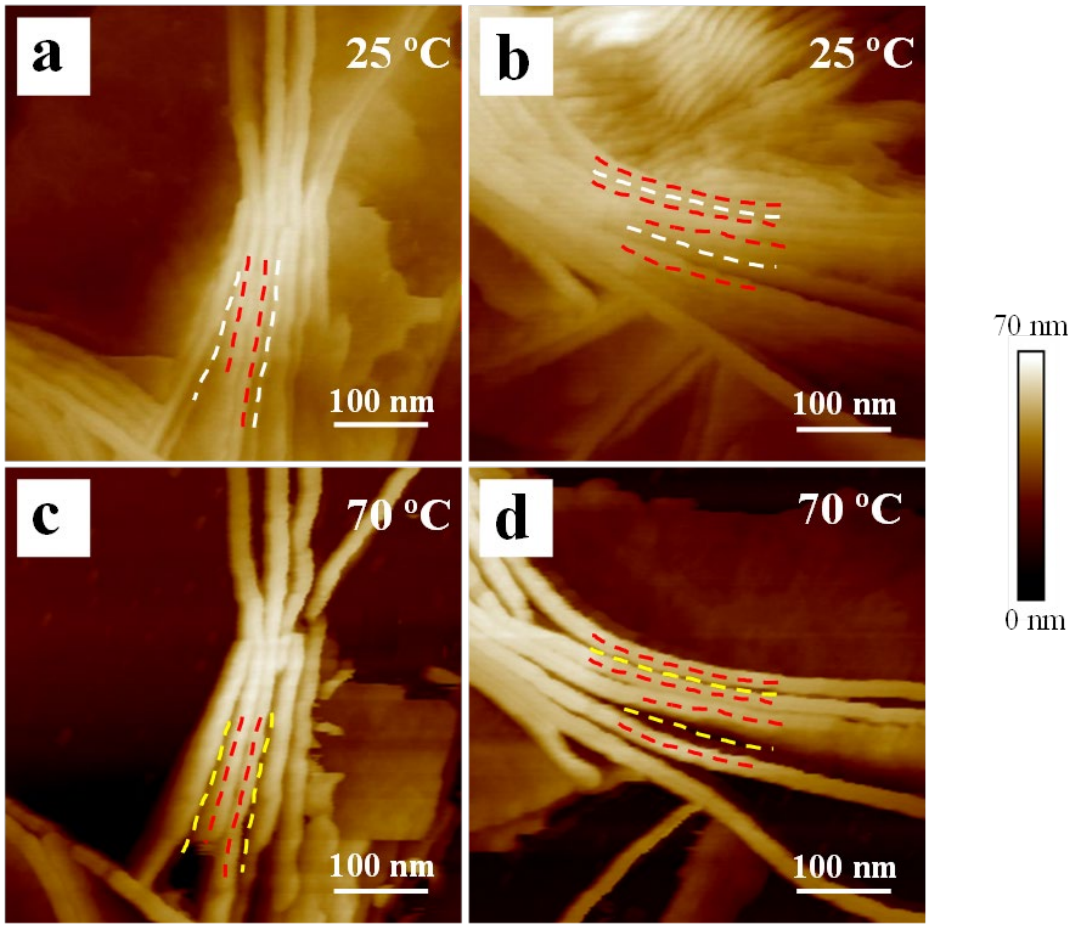

Figure 5. AFM height images of a $PEO_{23}PCL_{34}PLLA_{43}$[19.9] sample, initially prepared by spin-coating from a 0.2 wt% solution and then subjected to the thermal crystallization protocol indicated in Figure 1. Images are given at 25 ºC (a, b), and at 70 ºC (c, d) after heating. The dotted lines indicate PCL/PEO lamellae (white), PLLA lamellae (red) and molten PCL/PEO regions (yellow).

In the present work, we take advantage of the AFM experiments employing a Dimension Icon microscope equipped with a hot-stage. The $PEO_{23}PCL_{34}PLLA_{43}^{19.9}$ sample was crystallized, as explained in Figure 1, and then it was *in situ* slowly heated. Then, AFM images were registered at different temperatures on heating (i.e., 25 and 70 °C).

Figure 5 shows AFM height images of the triblock terpolymer. The aim is to identify the tri-lamellar structure of this multiphasic terpolymer. At 25 °C, it can be seen that some lamellae grew edge-on, while others are slightly tilted. This lamellar arrangement should include lamellae of the PLLA, PCL and PEO crystals. The WAXS experiment at 25 °C revealed the crystallographic planes of the three blocks (see Figure 6a).

Detailed measurements of the lamellar thickness at 25 °C (see Figure 5a and b) revealed two populations of different lamellar thickness. The thickest one is 17 ± 1 nm (red dotted line), and between these lamellae, another phase measures 11 ± 2 nm (white dotted lines). Comparing these values with those of the diblock copolymer, the thickness values of the bigger size lamellae are similar. Since the molecular weights of the PLLA blocks in both samples are alike and the crystallization conditions are the same, it is reasonable to assume that the 17 nm lamellae correspond to the PLLA block in the terpolymer.

Besides the 17 nm phase, the other one measured 11 nm (white dotted line). It is challenging to elucidate to which of the other two blocks correspond this phase. Increasing the temperature should melt one phase while keeping the other crystalline. It can be seen in Figure 6b and c that beyond 60 °C, only PLLA crystals remain. The effect of slowly increasing the temperature can be seen in the AFM images taken at 70 °C. At this temperature, both PEO and PCL crystals are molten. It is clear that the phase marked with

the white dotted line in Figure 5a and b disappeared in Figure 5c and d (signaled with a yellow dotted line).

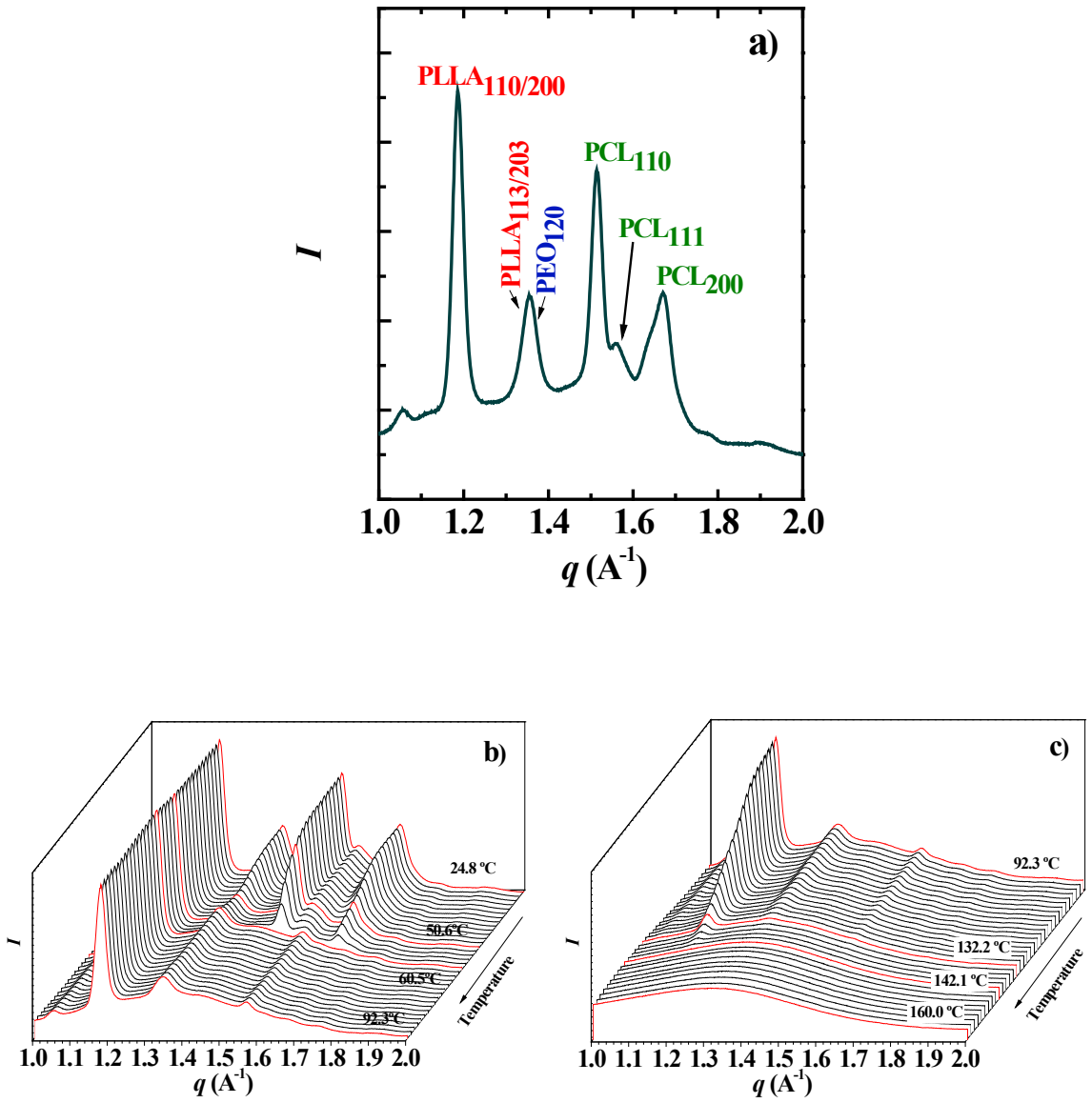

Figure 6. WAXS patterns of $PEO_{23}PCL_{34}PLLA_{43}^{19.9}$ diblock copolymer taken at 25 °C, after crystallizing the sample in two isothermal steps (a). WAXS patterns evolution of $PEO_{23}PCL_{34}PLLA_{43}^{19.9}$ during subsequent heating between 25 and 92 °C (b) and between 92 and 160 °C (c).

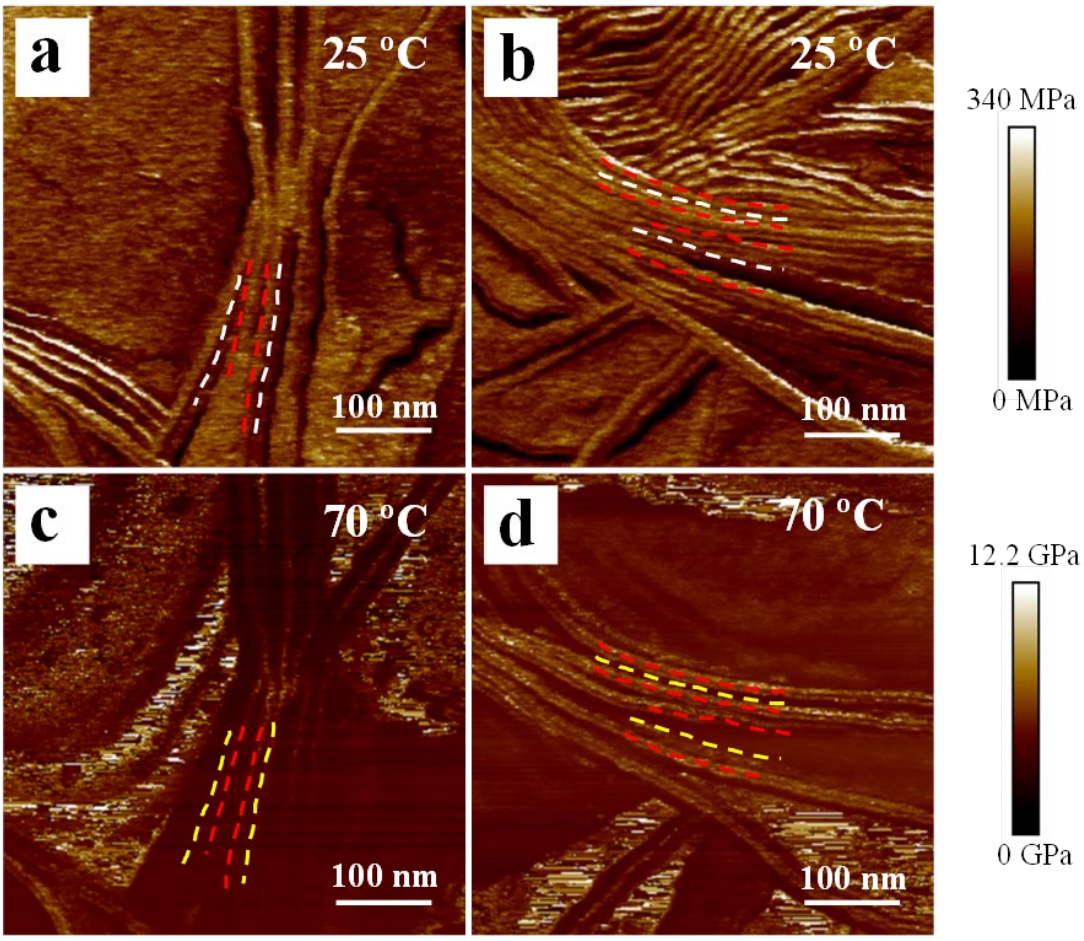

Figure 7. AFM modulus images of a $PEO_{23}PCL_{34}PLLA_{43}^{19.9}$ sample, initially prepared by spin-coating from a 0.2 wt% solution, and then subjected to the thermal crystallization protocol indicated in Figure 1. Images are given at 25 ºC (a, b), and at 70 ºC (c, d) after heating. The dotted lines indicate PCL/PEO lamellae (white), PLLA lamellae (red) and molten PCL/PEO regions (yellow).

Therefore, the AFM images allow confirming that the thickest lamellae (17 nm, red dotted line) belong to the PLLA crystals since these are the only lamellae remaining at 70 °C (a temperature above the melting point of both PEO and PCL blocks). The AFM modulus images also confirmed this observation (see Figure 7). The darker interlamellar region in-between the PLLA lamellae account for the softer amorphous phase resulting mainly from the molten PEO/PCL phase.

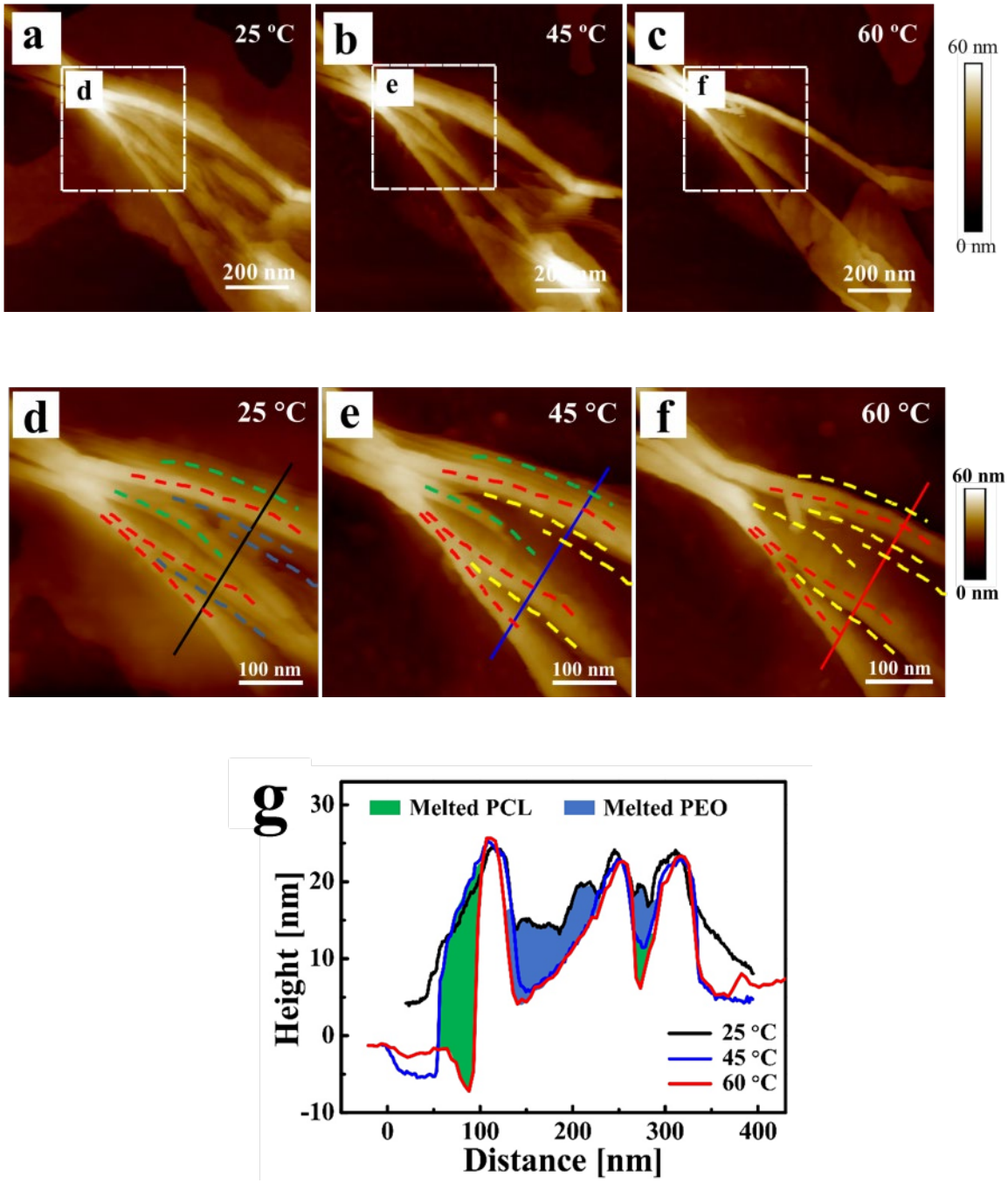

Figure 8. AFM height images of a $PEO_{23}PCL_{34}PLLA_{43}$[19.9] sample, initially prepared by spin-coating from a 0.1 wt% solution, and then subjected to the thermal crystallization protocol indicated in Figure 1. Images are given at 25 ºC (a, d), 45 ºC (b, e) and 60 ºC (c, f). The dotted lines indicate PEO lamellae (blue), PCL lamellae (green), PLLA lamellae (red), and the PEO/PCL melt region (yellow). (g) Cross-sectional height profiles along the directions indicated in Figure S2 in supplementary information. The green and blue regions of height reduction represent the melted PCL and PEO, respectively.

Nevertheless, trying to differentiate the PEO lamellae from the PCL lamellae from the images shown in Figure 7 for the $PEO_{23}PCL_{34}PLLA_{43}^{19.9}$ triblock terpolymer is more difficult than in the case of the diblock copolymer (Figure 4). Thus, to improve the quality of the AFM images, another sample solution of 0.5 wt% was prepared by spin-coating, and the film obtained melt crystallized as in Figure 1. Even though the sample solution was more concentrated, the multiphasic lamellar structure was not sufficiently clear in the AFM images taken with the Dimension Icon microscope (see Figure S2 and S3 in Supplementary Information), even after melting the samples. Therefore, the solution concentration was diluted down to 0.1 wt%, and the sample film was again crystallized following the same protocol described in Figure 1. After crystallization, the sample was slowly *in situ* heated, and AFM images were taken at 25, 45, and 60 °C. The sequence of AFM images on heating is presented in Figure 8 and Figure 9.

After employing a more diluted sample solution, the Dimension Icon AFM microscope confirms the multiphasic lamellar morphology that the authors hypothesized earlier [37]. An extraordinary view of the tri-lamellar arrangement is given by the AFM height images taken at 25 °C (see Figure 8a). Some of the lamellae are edge-on, and other lamellae are slightly tilted. After a closer observation and exhaustive measurements, three populations of different lamellar thickness were identified: 18 ± 1, 14 ± 1, and 10 ± 1 nm (see Figure 8d).

A clear trilayered morphology is observed at 25 °C. In Figure 8d, the thickest lamellae (i.e., 18 nm) are signaled with a red dotted line. While the intermediate size lamellae, with a green dotted line (i.e., 14 nm), and the thinnest lamellae (i.e., 10 nm) with a blue dotted. Thus, the premise is that each lamellae population might correspond to a

different crystalline phase: whether PLLA, PCL, or PEO. This hypothesis was only indirectly proven by WAXS analysis measurements in a previous publication [37]. In this report, we took advantage of the hot-stage AFM to determine to which phase belongs each lamella since each phase melts at different temperatures.

Under standard crystallization conditions, the PEO and PCL blocks in the $PEO_{23}PCL_{34}PLLA_{43}^{19.9}$ triblock terpolymer melt at approximately 45 and 54 °C, respectively, while the PLLA block does it at a much higher temperature, around 112-122 °C (see also Table 1) [35]. Figure 8b shows the AFM height image of the sample after heating to 45 °C. A closer observation (see Figure 8e) revealed the disappearance of the thinnest lamellae that were first marked with blue dotted lines. Since the PEO block melts at this temperature, the AFM height image proves undoubtedly that the thinnest lamellae belong to the PEO crystals. A yellow dotted line marks the position where the PEO lamellae were.

Further heating the sample up to 60 °C causes the melting of the PCL phase. The medium size lamellae, indicated with a green dotted line in Figure 8, have now disappeared while the thickest lamellae marked with the red dotted line remain (see Figure 8c and f). At that temperature, only the PLLA block is crystalline, while the other two are completely molten.

The AFM images upon sequential heating confirm that the 14 nm lamellae are PCL block lamellar crystals, and the 18 nm lamellae correspond to the PLLA block. The exact position of where PCL lamellae were has been marked with yellow dotted lines in Figure 8f, while the lamellae that remain correspond to the PLLA block. The trilayered

morphology has been confirmed, and the $PEO_{23}PCL_{34}PLLA_{43}^{19.9}$ triblock terpolymer can be prepared as a truly multi-crystalline system, provided suitable crystallization conditions are applied.

As in the diblock copolymer, cross-sectional height profiles yield valuable information that can be used to identify the lamellar melting sequence of the $PEO_{23}PCL_{34}PLLA_{43}^{19.9}$, as shown in Figure 8g (see solid black, blue and red line in Figure 8d-f to observe the marked section where the measurements were taken). At 25 °C, multiple peaks and valleys are present (see black line) that correspond to the existing lamellar populations. The highest peaks correspond to the PLLA block that has the thickest lamellae. As the temperature increased up to 45 °C, some zones and peaks in the profile remained unchanged (see blue line) while new valleys of reduced height appear. In other words, the zones marked in blue disappeared. This reduction accounts for the melting of PEO lamellae since at 45 ºC this block is molten. Further increment of the temperature up to 60 °C caused the disappearance of other zones while the main peaks remain invariable (see red line). These zones, colored in green, represented the PCL lamellae that were crystalline at 45 °C but completely molten at 60 °C. Although less clear, the multiphasic nanoscale morphology was also observed through AFM modulus images. Figure 9 shows the lamellar structure of the $PEO_{23}PCL_{34}PLLA_{43}^{19.9}$ triblock terpolymer at different temperatures. It could be difficult to elucidate each phase by taking into account the mechanical modulus only.

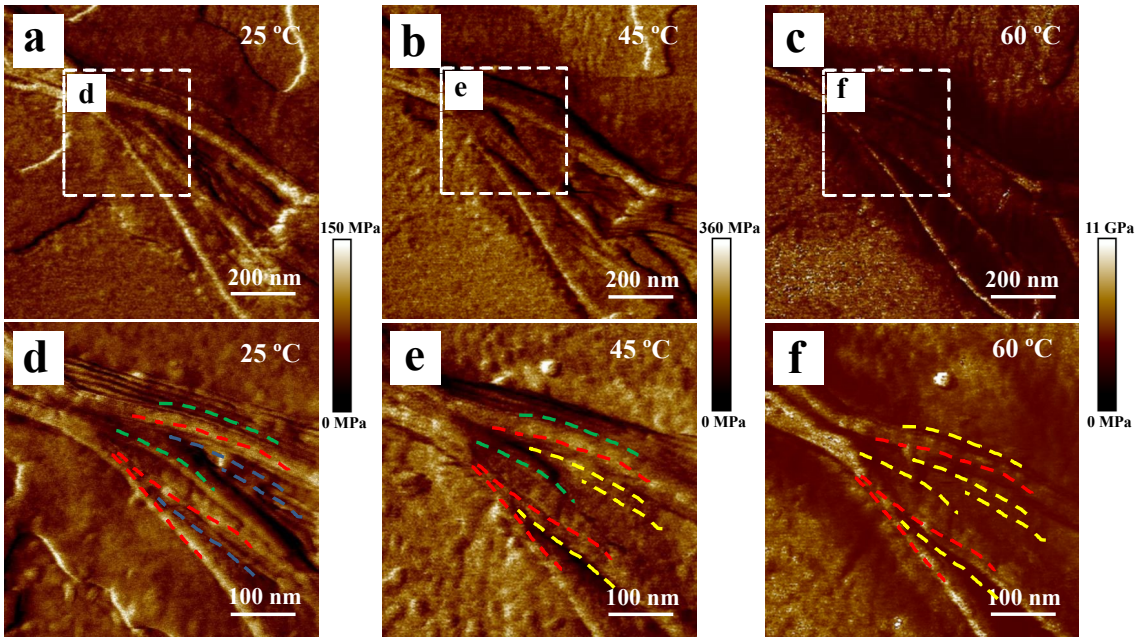

Figure 9. AFM modulus images of a $PEO_{23}PCL_{34}PLLA_{43}$[19.9] sample, originally prepared by spin-coating from a 0.1 wt% solution, and then subjected to the thermal crystallization protocol indicated in Figure 1. Images are given at 25 ºC (a, b), 45 ºC (b, c) and 60 ºC (d, e). The dotted lines indicate PEO lamellae (blue), PCL lamellae (green), PLLA lamellae (red), and the PEO/PCL melt region (yellow).

Even though the PLLA is a more rigid material, while the PCL and PEO are softer polymers, it is complicated to differentiate them in the AFM modulus images at 25 °C (see Figure 9a and d). The reason is probably that PCL and PEO have comparable mechanical properties [67, 70]. However, as the sample is heated to 45 and 60 °C, some lamellae disappeared while others remained brighter. Since the amorphous phase is a softer one, the mechanical modulus is lower as a result of the melting of the PCL and PEO crystals (darker areas). Therefore, at 60 °C, only the rigid-higher modulus crystalline phase of the PLLA block is observed, surrounded by a darker area (signaled with yellow dotted lines) that correspond to the melt mixed amorphous PCL/PEO phase.

Besides elucidating the nanoscale morphology, the hot-stage AFM technique and cross-sectional height profiles measurements are useful to ascertain the details of how the three types of lamellae in the triblock terpolymer arrange. In our previous publication [37],an exhaustive theoretical analysis of SAXS characterization upon heating suggested that only one lamella of either PEO or PCL randomly inserts between two adjacent PLLA lamellae. This premise was proposed after modeling SAXS theoretical curves considering a one-dimensional structural model. The AFM images and the cross-sectional height profiles exhibited in Figure 8 support this premise, since we could observed PLLA interlamellar zones occupied by PCL or PEO only. For instance, it is possible to observe only one lamella of PEO in between two lamellae of PLLA (blue dotted line in Figure 8d and middle blue zone in Figure 8g).

However, the nanoscale structure observed in Figure 8a and d provided an additional lamellar arrangement, previously undetected. In Figure 8d, it can be observed that some lamellae of both PCL and PEO (green and blue dotted lines) intercalate between two lamellae of PLLA (red dotted lines). Also, some evidences of intercalated PEO and PCL lamellae can be observed in the cross-sectional height profiles. Therefore, these new evidences, gathered by hot-stage AFM, suggest that the complex morphology of the PEO-*b*-PCL-*b*-PLLA triblock terpolymers under investigation can also include regions where the order of lamellar positioning can also be described as exact interdigitation, i.e., PLLA/PEO/PCL/PLLA, instead of only the random intercalation of one PCL or one PEO lamellae in between two PLLA lamellae, i.e., PLLA/PEO/PLLA or PLLA/PCL/PLLA at random.

Despite this observation, it should be considered that the SAXS analysis is a broader range technique that can assess the structural features of the system in bulk. On the contrary, the AFM technique is a surface characterization tool that scans a very particular area of the sample surface and, therefore, might not represent the entire sample. What is significant is that the Dimension Icon AFM microscope not only showed to some extent the random lamellar arrangement proposed earlier [37], but in addition, it gives clear evidence of the multi-crystalline morphology of triple crystalline PEO-*b*-PCL-*b*-PLLA triblock terpolymers. To our knowledge, this is the first time that hot-stage AFM is used to provide an accurate description of the nanoscale morphology of ABC type triblock terpolymer with three crystalline phases.

CONCLUSIONS

The hot-stage atomic force microscopy (AFM) has been used to accurately determine the tri-crystalline tri-layered morphology of a PEO-*b*-PCL-*b*-PLLA triblock terpolymer for the first time. This ABC type triblock terpolymer is melt miscible, and the three blocks can crystallize sequentially upon cooling from the melt, as confirmed by WAXS. A two-step crystallization protocol was applied to the PEO-*b*-PCL-*b*-PLLA triblock terpolymer and to an analogous PCL-*b*-PLLA diblock copolymer for comparison purposes. A clear lamellar self-assembly, including lamellae of different lamellar thickness, was observed by AFM at room temperature.

Considering the differences between the melting temperatures of the blocks, the sequential melting of the PEO-*b*-PCL-*b*-PLLA sample in the hot-stage allowed

undoubtedly assigning the three crystalline lamellar thickness populations observed in the AFM images. This was done thanks to the great advantages of the AFM technique employed that allow: 1. Detailed morphological observations at different temperatures (as the samples underwent sequential melting), 2. Cross-sectional height measurements at different temperatures to distinguished the different lamellar types and 3. Determination of mechanical properties of the different lamellae as a function of temperature.

The thickest lamellae belong to the PLLA block, the medium size lamellae to the PCL block, and the thinnest lamellae to the PEO block. The lamellar self-assembly includes exact interdigitation of the 3 types of lamellae in sequence (i.e., PLLA/PEO/PCL/PLLA) or the intercalation at random of one PCL or one PEO lamellae in between two PLLA lamellae. The hot-stage AFM is a valuable technique to elucidate the complex nanoscale lamellar morphology of multi-crystalline systems.

ACKNOWLEDGMENTS

We would like to thank the financial support provided by the BIODEST project. This project has received funding from the European Union's Horizon 2020 research and innovation programme under the Marie Skłodowska-Curie grant agreement No 778092. We also ackwoledge funding from MINECO, project: MAT2017-83014-C2-1-P and from the Basque Government through grant IT1309-19. We are grateful to the National Science Foundation of China (nos. 51773182, 51973202), The Young Out-standing Teachers of the University in Henan Province (2019GGJS003). N.H. acknowledges the support of King Abdullah University of Science and Technology (KAUST).

REFERENCES

[1] I.W. Hamley, Block Copolymers, Encyclopedia of Polymer Science and Technology, John Wiley & Sons, Inc.2002, pp. 457-482.

[2] S. Huang, S. Jiang, Structures and morphologies of biocompatible and biodegradable block copolymers, RSC Advances 4(47) (2014) 24566-24583.

[3] S. Nojima, H. Marubayashi, Crystalline Morphology of Homopolymers and Block Copolymers, in: Q. Guo (Ed.), Polymer Morphology: Principles, Characterization, and Processing, John Wiley & Sons, Inc, Hoboken, NJ, 2016, pp. 165-180.

[4] J.K. Palacios, A. Mugica, M. Zubitur, A.J. Müller, Crystallization and morphology of block copolymers and terpolymers with more than one crystallizable block, Crystallization in Multiphase Polymer Systems2018, pp. 123-180.

[5] A.J. Müller, M.L. Arnal, A.T. Lorenzo, Crystallization in Nano-Confined Polymeric Systems, in: E. Piorkowska, G.C. Rutledge (Eds.), Handbook of Polymer Crystallization, John Wiley and Sons, Hoboken, New Jersey, 2013, pp. 347-372.

[6] A.J. Müller, M.L. Arnal, V. Balsamo, Crystallization in block copolymers with more than one crystallizable block, Lecture Notes in Physics 714 (2007) 229-259.

[7] A.J. Müller, V. Balsamo, M.L. Arnal, Nucleation and crystallization in diblock and triblock copolymers, Adv. Polym. Sci. 190 (2005) 1-63.

[8] S.N. Magonov, Atomic Force Microscopy in Analysis of Polymers, Encyclopedia of Analytical Chemistry (2006) 1-58.

[9] H. Schönherr, G.J. Vancso, Scanning Force Microscopy of Polymers, Springer, Verlag Berlin Heidelberg, 2010.

[10] H. Schönherr, Imaging Polymer Morphology using Atomic Force Microscopy, in: Q. Guo (Ed.), Polymer Morphology: Principles, Characterization, and Processing, John Wiley & Sons, Inc, Hoboken, NJ, 2016, pp. 100-117.

[11] S. Ludwigs, K. Schmidt, C.M. Stafford, E.J. Amis, M.J. Fasolka, A. Karim, R. Magerle, G. Krausch, Combinatorial mapping of the phase behavior of ABC triblock terpolymers in thin films: Experiments, Macromolecules 38 (2005) 1850-1858.

[12] M. Zerson, M. Neumann, R. Steyrleuthner, D. Neher, R. Magerle, Surface structure of semicrystalline naphthalene Diimide−Bithiophene copolymer films studied with atomic force microscopy, Macromolecules 49 (2016) 6549−6557.

[13] R.V. Castillo, A.J. Müller, Crystallization and morphology of biodegradable or biostable single and double crystalline block copolymers, Prog. Polym. Sci. 34(6) (2009) 516-560.

[14] W.N. He, J.T. Xu, Crystallization assisted self-assembly of semicrystalline block copolymers, Prog. Polym. Sci. 37(10) (2012) 1350-1400.

[15] S. Nakagawa, H. Marubayashi, S. Nojima, Crystallization of polymer chains confined in nanodomains, Eur. Polym. J. 70 (2015) 262-275.

[16] Y.L. Loo, R.A. Register, A.J. Ryan, Modes of crystallization in block copolymer microdomains: Breakout, templated, and confined, Macromolecules 35(6) (2002) 2365-2374.

[17] A. Boschetti-De-Fierro, D. Fierro, J. Albuerne, S.S. Funari, V. Abetz, Thermal monitoring of morphology in triblock terpolymers with crystallizable blocks, J. Polym. Sci., Part B: Polym. Phys. 45(23) (2007) 3197-3206.

[18] A.J. Müller, J. Albuerne, L. Marquez, J.M. Raquez, P. Degée, P. Dubois, J. Hobbs, I.W. Hamley, Self-nucleation and crystallization kinetics of double crystalline poly(p-dioxanone)-b-poly(ε-caprolactone) diblock copolymers, Faraday Discuss. 128 (2005) 231-252.

[19] A.J. Müller, J. Albuerne, L.M. Esteves, L. Marquez, J.M. Raquez, P. Degée, P. Dubois, S. Collins, I.W. Hamley, Confinement effects on the crystallization kinetics and self-nucleation of double crystalline poly(p-dioxanone)-b-poly(ε-caprolactone) diblock copolymers, Macromol. Sym., 2004, pp. 369-382.

[20] J. Albuerne, L. Márquez, A.J. Müller, J.M. Raquez, P. Degée, P. Dubois, V. Castelletto, I.W. Hamley, Nucleation and crystallization in double crystalline poly(p-dioxanone)-b-poly(ε-caprolactone) diblock copolymers, Macromolecules 36(5) (2003) 1633-1644.

[21] M.L. Arnal, V. Balsamo, F. López-Carrasquero, J. Contreras, M. Carrillo, H. Schmalz, V. Abetz, E. Laredo, A.J. Müller, Synthesis and characterization of polystyrene-b-poly(ethylene oxide)-b-poly(ε-caprolactone) block copolymers, Macromolecules 34(23) (2001) 7973-7982.

[22] V. Balsamo, Y. Paolini, G. Ronca, A.J. Müller, Crystallization of the polyethylene block in polystyrene-b-polyethylene-b-polycaprolactone triblock copolymers, 1: Self-nucleation behavior, Macromol. Chem. Phys. 201(18) (2000) 2711-2720.

[23] V. Balsamo, A.J. Müller, R. Stadler, Antinucleation effect of the polyethylene block on the polycaprolactone block in ABC triblock copolymers, Macromolecules 31(22) (1998) 7756-7763.

[24] V. Balsamo, A.J. Müller, F. Von Gyldenfeldt, R. Stadler, Ternary ABC block copolymers based on one glassy and two crystallizable blocks: Polystyrene-block-polyethylene-block-poly(ε-caprolactone), Macromol. Chem. Phys. 199(6) (1998) 1063-1070.

[25] M.L. Arnal, S. Boissé, A.J. Müller, F. Meyer, J.M. Raquez, P. Dubois, R.E. Prud'Homme, Interplay between poly(ethylene oxide) and poly(l-lactide) blocks during diblock copolymer crystallization, CrystEngComm 18(20) (2016) 3635-3649.

[26] S. Huang, S. Jiang, L. An, X. Chen, Crystallization and morphology of poly(ethylene oxide-b-lactide) crystalline-crystalline diblock copolymers, J. Polym. Sci., Part B: Polym. Phys. 46(13) (2008) 1400-1411.

[27] Y. Li, H. Huang, Z. Wang, T. He, Tuning radial lamellar packing and orientation into diverse ring-banded spherulites: Effects of structural feature and crystallization condition, Macromolecules 47(5) (2014) 1783-1792.

[28] F. Xue, X. Chen, L. An, S.S. Funari, S. Jiang, Soft nanoconfinement effects on the crystallization behavior of asymmetric poly(ethylene oxide)-block-poly(ε- caprolactone) diblock copolymers, Polym. Int. 61(6) (2012) 909-917.

[29] C. He, J. Sun, J. Ma, X. Chen, X. Jing, Composition dependence of the crystallization behavior and morphology of the poly(ethylene oxide)-poly(ε-caprolactone) diblock copolymer, Biomacromolecules 7(12) (2006) 3482-3489.

[30] S. Jiang, C. He, L. An, X. Chen, B. Jiang, Crystallization and ring-banded spherulite morphology of poly(ethylene oxide)-block-poly(ε-caprolactone) diblock copolymer, Macromol. Chem. Phys. 205(16) (2004) 2229-2234.

[31] W. Han, X. Liao, Q. Yang, G. Li, B. He, W. Zhu, Z. Hao, Crystallization and morphological transition of poly(l-lactide)-poly(?-caprolactone) diblock copolymers with different block length ratios, RSC Advances 7(36) (2017) 22515-22523.

[32] S. Huang, H. Li, S. Jiang, X. Chen, L. An, Morphologies and structures in poly(l-lactide-b-ethylene oxide) copolymers determined by crystallization, microphase separation, and vitrification, Polym. Bull. 67(5) (2011) 885-902.

[33] J.L. Wang, C.M. Dong, Synthesis, sequential crystallization and morphological evolution of well-defined star-shaped poly(ε-caprolactone)-b-poly(L-lactide) block copolymer, Macromol. Chem. Phys. 207(5) (2006) 554-562.

[34] J. Sun, Z. Hong, L. Yang, Z. Tang, X. Chen, X. Jing, Study on crystalline morphology of poly(L-lactide)-poly(ethylene glycol) diblock copolymer, Polymer 45(17) (2004) 5969-5977.

[35] J.K. Palacios, A. Mugica, M. Zubitur, A. Iturrospe, A. Arbe, G. Liu, D. Wang, J. Zhao, N. Hadjichristidis, A.J. Muller, Sequential crystallization and morphology of triple crystalline biodegradable PEO-b-PCL-b-PLLA triblock terpolymers, RSC Advances 6(6) (2016) 4739-4750.

[36] J.K. Palacios, G. Liu, D. Wang, N. Hadjichristidis, A.J. Müller, Generating Triple Crystalline Superstructures in Melt Miscible PEO-b-PCL-b-PLLA Triblock Terpolymers by Controlling Thermal History and Sequential Crystallization, Macromol. Chem. Phys. 220(20) (2019) 1900292.

[37] J.K. Palacios, A. Tercjak, G. Liu, D. Wang, J. Zhao, N. Hadjichristidis, A.J. Müller, Trilayered Morphology of an ABC Triple Crystalline Triblock Terpolymer, Macromolecules 50(18) (2017) 7268-7281.

[38] J.K. Palacios, J. Zhao, N. Hadjichristidis, A.J. Müller, How the Complex Interplay between Different Blocks Determines the Isothermal Crystallization Kinetics of Triple-Crystalline PEO-b-PCL-b-PLLA Triblock Terpolymers, Macromolecules 50(24) (2017) 9683-9695.

[39] Y.-W. Chiang, Y.-Y. Hu, J.-N. Li, S.-H. Huang, S.-W. Kuo, Trilayered Single Crystals with Epitaxial Growth in Poly(ethylene oxide)-block-poly(ε-caprolactone)-block-poly(l-lactide) Thin Films, Macromolecules 48(23) (2015) 8526-8533.

[40] R. Liénard, N. Zaldua, T. Josse, J.D. Winter, M. Zubitur, A. Mugica, A. Iturrospe, A. Arbe, O. Coulembier, A.J. Müller, Synthesis and Characterization of Double Crystalline Cyclic Diblock Copolymers of Poly(ε-caprolactone) and Poly(l(d)-lactide) (c(PCL-b-PL(D)LA)), Macromol. Rapid Commun. 37(20) (2016) 1676-1681.

[41] R.V. Castillo, A.J. Müller, J.M. Raquez, P. Dubois, Crystallization kinetics and morphology of biodegradable double crystalline PLLA- b -PCL diblock copolymers, Macromolecules 43(9) (2010) 4149-4160.

[42] I.W. Hamley, P. Parras, V. Castelletto, R.V. Castillo, A.J. Müller, E. Pollet, P. Dubois, C.M. Martin, Melt structure and its transformation by sequential crystallization of the two blocks within poly(L-lactide)-block-poly(ε-caprolactone) double crystalline diblock copolymers, Macromol. Chem. Phys. 207(11) (2006) 941-953.

[43] C. Cai, L.U. Wang, C.M. Donc, Synthesis, characterization, effect of architecture on crystallization, and spherulitic growth of poly(L-lactide)b-poly(ethylene oxide) copolymers with different branch arms, J. Polym. Sci., Part A: Polym. Chem. 44(6) (2006) 2034-2044.

[44] I.W. Hamley, V. Castelletto, R.V. Castillo, A.J. Müller, C.M. Martin, E. Pollet, P. Dubois, Crystallization in poly(L-lactide)-b-poly(ε-caprolactone) double crystalline diblock

copolymers: A study using x-ray scattering, differential scanning calorimetry, and polarized optical microscopy, Macromolecules 38(2) (2005) 463-472.

[45] D. Shin, K. Shin, K.A. Aamer, G.N. Tew, T.P. Russell, J.H. Lee, J.Y. Jho, A morphological study of a semicrystalline poly(L-lactic acid-b-ethylene oxide-b-L-lactic acid) triblock copolymer, Macromolecules 38(1) (2005) 104-109.

[46] S.G. Prilliman, A.M. Kavanagh, E.C. Scher, S.T. Robertson, K.S. Hwang, V.L. Colvin, An in-situ hot stage for temperature-dependent tapping-mode™ atomic force microscopy, Rev. Sci. Instrum. 69(9) (1998) 3245-3250.

[47] B. Zhang, J. Chen, P. Freyberg, R. Reiter, R. Mülhaupt, J. Xu, G. Reiter, High-Temperature Stability of Dewetting-Induced Thin Polyethylene Filaments, Macromolecules 48(5) (2015) 1518-1523.

[48] B. Zhang, J. Chen, M.C. Baier, S. Mecking, R. Reiter, R. Mulhaupt, G. Reiter, Molecular-weight-dependent changes in morphology of solution-grown polyethylene single crystals, Macromol Rapid Commun 36(2) (2015) 181-9.

[49] B. Zhang, J. Chen, H. Zhang, M.C. Baier, S. Mecking, R. Reiter, R. Mülhaupt, G. Reiter, Annealing-induced periodic patterns in solution grown polymer single crystals, RSC Advances 5(17) (2015) 12974-12980.

[50] C.-d. Qiao, S.-c. Jiang, X.-l. Ji, L.-j. An, In situ observation of melting and crystallization behaviors of poly(ε-caprolactone) ultra-thin films by AFM technique, Chin. J. Polym. Sci. 31(9) (2013) 1321-1328.

[51] V.H. Mareau, R.E. Prud'homme, In-Situ Hot Stage Atomic Force Microscopy Study of Poly(ε-caprolactone) Crystal Growth in Ultrathin Films, Macromolecules 38(2) (2005) 398-408.

[52] E. Núñez, G.J. Vancso, U.W. Gedde, Morphology, crystallization, and melting of single crystals and thin films of star-branched polyesters with poly(-caprolactone) arms as revealed by atomic force microscopy, Journal of Macromolecular Science, Part B: Physics 47(3) (2008) 589-607.

[53] L.G.M. Beekmans, D.W. Van der Meer, G.J. Vancso, Crystal melting and its kinetics on poly(ethylene oxide) by in situ atomic force microscopy, Polymer 43(6) (2002) 1887-1895.

[54] E.Q. Chen, A.J. Jing, X. Weng, P. Huang, S.W. Lee, S.Z.D. Cheng, B.S. Hsiao, F. Yeh, In situ observation of low molecular weight poly(ethylene oxide) crystal melting, recrystallization, Polymer 44(19) (2003) 6051-6058.

[55] H. Schönherr, C.W. Frank, Ultrathin films of poly(ethylene oxides) on oxidized silicon. 2. In situ study of crystallization and melting by hot stage AFM, Macromolecules 36(4) (2003) 1199-1208.

[56] X. Jiang, X. Liu, Q. Liao, X. Wang, D.D. Yan, H. Huo, L. Li, J.J. Zhou, Probing interfacial properties using a poly(ethylene oxide) single crystal, Soft Matter 10(18) (2014) 3238-3244.

[57] H. Wang, J.M. Schultz, S. Yan, Study of the morphology of poly(butylene succinate)/poly(ethylene oxide) blends using hot-stage atomic force microscopy, Polymer 48(12) (2007) 3530-3539.

[58] Y. Huang, X.B. Liu, H.L. Zhang, D.S. Zhu, Y.J. Sun, S.K. Yan, J. Wang, X.F. Chen, X.H. Wan, E.Q. Chen, Q.F. Zhou, AFM study of crystallization and melting of a poly(ethylene oxide) diblock copolymer containing a tablet-like block of poly{2,5-bis[(4-methoxyphenyl) oxycarbonyl]styrene} in ultrathin films, Polymer 47(4) (2006) 1217-1225.

[59] P. Zhang, Z. Wang, H. Huang, T. He, Direct observation of the relief structure formation in the nearly symmetric poly(styrene)-block-poly(ε-caprolactone) diblock copolymer thin film, Macromolecules 45(22) (2012) 9139-9146.

[60] D. Cui, T. Tang, W. Bi, J. Cheng, W. Chen, B. Huang, Ring-opening polymerization and block copolymerization of L-lactide with divalent samarocene complex, J. Polym. Sci., Part A: Polym. Chem. 41(17) (2003) 2667-2675.

[61] H. Schmalz, A. Knoll, A.J. Müller, V. Abetz, Synthesis and characterization of ABC triblock copolymers with two different crystalline end blocks: Influence of confinement on crystallization behavior and morphology, Macromolecules 35(27) (2002) 10004-10013.

[62] H. Alamri, J. Zhao, D. Pahovnik, N. Hadjichristidis, Phosphazene-catalyzed ring-opening polymerization of ε -caprolactone: influence of solvents and initiators, Polym. Chem. 5(18) (2014) 5471-5478.

[63] J. Zhao, D. Pahovnik, Y. Gnanou, N. Hadjichristidis, Sequential polymerization of ethylene oxide, ε-caprolactone and l-lactide: A one-pot metal-free route to tri- and pentablock terpolymers, Polym. Chem. 5(12) (2014) 3750-3753.

[64] R.M. Ho, P.Y. Hsieh, W.H. Tseng, C.C. Lin, B.H. Huang, B. Lotz, Crystallization-Induced Orientation for Microstructures of Poly(L-lactide)-b-poly(ε-caprolactone) Diblock Copolymers, Macromolecules 36(24) (2003) 9085-9092.

[65] M.T. Casas, J. Puiggalí, J.M. Raquez, P. Dubois, M.E. Córdova, A.J. Müller, Single crystals morphology of biodegradable double crystalline PLLA-b-PCL diblock copolymers, Polymer 52(22) (2011) 5166-5177.

[66] S. Fiori, Industrial Uses of PLA, in: A. Jimenez, M. Peltzer, R. Ruseckaite (Eds.), Poly(lactic acid) Science and Technology: Processing, Properties, Additives and Applications, The Royal Society of Chemistry, Cambridge, 2015, pp. 317-333.

[67] G. Cama, D.E. Mogosanu, A. Houben, P. Dubruel, Synthetic biodegradable medical polyesters: Poly-ε-caprolactone, in: X. Zhang (Ed.), Science and Principles of Biodegradable and Bioresorbable Medical Polymers, Woodhead Publishing2017, pp. 79-105.

[68] H. Zhou, G.L. Wilkes, Comparison of lamellar thickness and its distribution determined from d.s.c., SAXS, TEM and AFM for high-density polyethylene films having a stacked lamellar morphology, Polymer 38(23) (1997) 5735-5747.

[69] D. Trifonova, J. Varga, G.J. Vancso, AFM study of lamellar thickness distributions in high temperature melt-crystallization of β-polypropylene, Polym. Bull. 41(3) (1998) 341-348.

[70] D.M. Back, R.L. Schmitt, Ethylene Oxide Polymers, Encyclopedia of Polymer Science and Technology, John Wiley & Sons, Inc.2002.